



# CHORUS

This is the accepted manuscript made available via CHORUS. The article has been published as:

## Bistable and Self-Tunable Negative-Index Metamaterial at Optical Frequencies

Pai-Yen Chen, Mohamed Farhat, and Andrea Alù

Phys. Rev. Lett. **106**, 105503 — Published 8 March 2011

DOI: [10.1103/PhysRevLett.106.105503](https://doi.org/10.1103/PhysRevLett.106.105503)

# ***Bistable and Self-Tunable Negative Index Metamaterial at Optical Frequencies***

Pai-Yen Chen<sup>\*</sup>, Mohamed Farhat<sup>†</sup>, and Andrea Alù<sup>‡</sup>

*Department of Electrical and Computer Engineering, The University of Texas at  
Austin, Austin, TX, 78712, USA.*

*We introduce a metamaterial design composed of square plasmonic loops loaded by Kerr nonlinearities that combines enhanced nonlinear response with strong artificial magnetism, ensuring negative refractive index with bistable and self-tunable response. We verify with full-wave simulations that positive-to-negative switching of refractive index may be obtained with moderate loss. The design of a finite-size metamaterial prism is also presented, supporting at the same frequency and for same light intensity positive or inverted Snell refraction as a function of its previous excitation history.*

PACS numbers: 81.05.Xj, 78.67.Pt, 81.05.Xj, 41.20.Jb

After their first realization at microwave frequencies [1], negative-index metamaterials (NIM) [2] have been at the center of significant interest in the physics and engineering communities, due to their exotic electromagnetic properties and their fascinating applications. Since then, significant efforts have

---

<sup>\*</sup> Email: pychen@mail.utexas.edu

<sup>†</sup> Email: mohamed.farhat@fresnel.fr

<sup>‡</sup> To whom correspondence should be addressed. Email: alu@mail.utexas.edu

been spent to realize low-loss negative-index of refraction at optical frequencies [3], as some of the most intriguing applications of these artificial materials, in particular sub-wavelength imaging [4] and cloaking [5], may revolutionize current technology when reliably realized in the visible. Although negative refraction of light from a planar interface may be obtained using photonic crystals [6], ‘true’ negative index of refraction and its anomalous properties are obtained in a composite material by inducing local negative effective permittivity and permeability in the same frequency window [2]. This requires that the metamaterial granularity is significantly smaller than the wavelength, and that loss mechanisms are moderate. Although negative permittivity is naturally available in the visible using plasmonic materials [7], the optical magnetism of natural materials is very weak [8] and artificial magnetic effects based on circulating conduction currents, successfully employed at lower frequencies, saturate above THz frequencies [9]. Alternative routes to optical artificial magnetism involve the use of plasmonic composite materials, often accompanied by severe loss effects and an inclusion size not necessarily small compared to the wavelength [10]. In this context, Alù and Engheta have shown that a loop of plasmonic nanoparticles may produce strong magnetic response at optical frequencies, possibly accompanied by negative effective permittivity in the same frequency range [11]. This geometry has been shown to provide a viable way towards negative index optical metamaterials with moderate losses, since loops with even numbers of nanoparticles inherently cancel unwanted quadrupolar radiation from the inclusions, at the basis of significant loss effects in other

geometries. For simplicity of analysis, in [11] the nanoloop consisted of plasmonic metal spheres, but other geometries may provide superior performance in terms of robustness to loss and bandwidth of operation [12].

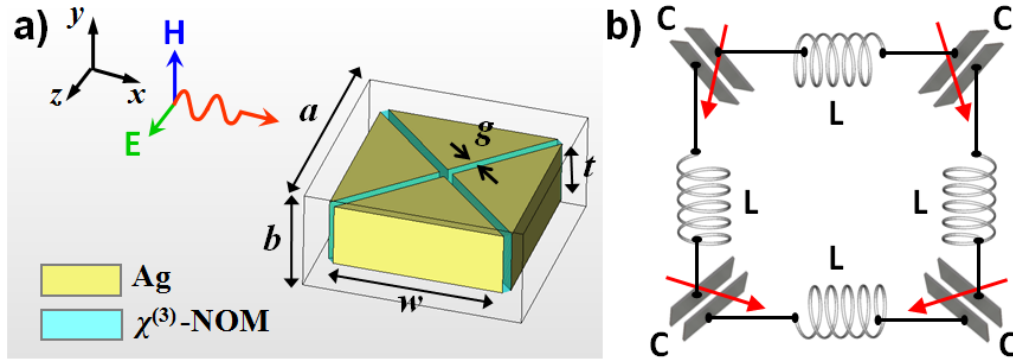


Figure 1 – (Color online) (a) Geometry of interest: a square-loop loaded by nonlinear optical materials; (b) Its equivalent nanocircuit model

In the following, we consider a variation of this nanoloop geometry that may realize not only low-loss negative index of refraction, but also add strong nonlinear, self-tunable response with bistable properties. Tunable and nonlinear properties are currently one of the most exciting areas of metamaterial research [13], since they may add a large degree of control and flexibility to the exotic properties of metamaterials. Various metamaterial geometries with nonlinear response have been investigated at microwave and optical frequencies [14], and tunable magnetic response using nonlinearities has been explored at microwave and THz frequencies [15]. Here, we combine the strong electric and magnetic resonance response of the nanoloop geometry with the nonlinear properties of Kerr optical materials to realize bistable and self-tunable positive to negative index of refraction in the visible. Since the typical size of metamaterial inclusions

and the naturally available nonlinear effects of optical materials are both inherently limited, available negative-index metamaterial geometries may not be able to provide sufficient nonlinear response within reasonable levels of optical intensity to produce these effects. For this reason, we introduce here a novel plasmonic inclusion, depicted in Fig. 1a, that may drastically enhance the nonlinear optical response, and at the same time improve the robustness of the nanoloop geometry. The structure is composed of a metal square parallelepiped with side  $w$  and thickness  $t$  cut across the diagonals with two narrow slits of width  $g$ , loaded by a material with relative permittivity  $\epsilon_L$  in its linear regime. The plasmonic square-loop is embedded in a glass host medium with relative permittivity  $\epsilon_h = 2.25$ . Also this geometry can support a circulating displacement current, but, superior to the nanoloop geometry [11], the presence of elongated tiny gaps introduces large and controllable capacitance values

$$C = \epsilon_L \epsilon_0 \frac{wt}{\sqrt{2}g}, \quad (1)$$

which may resonate in series with the inductance of the plasmonic segments, consistent with its equivalent nanocircuit [16] model in Fig. 1b. As a result, a strong circulating displacement current may sustain the magnetic resonance of this inclusion, weakly dependent on its overall size, but instead based on its plasmonic properties [11]. This is shown in the inset of Fig. 2a, where the electric field distribution at the magnetic resonance of this loop (at frequency  $f_0 = 490$  THz) is reported for plane wave excitation with magnetic field polarized along the axis of the loop and  $w = 100$  nm,  $t = 35$  nm,  $a = 110$  nm,  $b = 50$  nm,  $g = 5$  nm,

$\epsilon_L = 2$ . In our simulations, we have considered silver for the square-loop material, modeled with a Drude-type permittivity as  $\epsilon(\omega) = \epsilon_\infty - \frac{\omega_p^2}{\omega^2 + i\gamma\omega}$ , with  $\omega_p / 2\pi = 2175\text{THz}$ ,  $\gamma / 2\pi = 4.35\text{THz}$  and  $\epsilon_\infty = 5$  [17], taking into account the frequency dispersion and absorption at optical frequencies. Further details of our numerical approach are provided in [18].

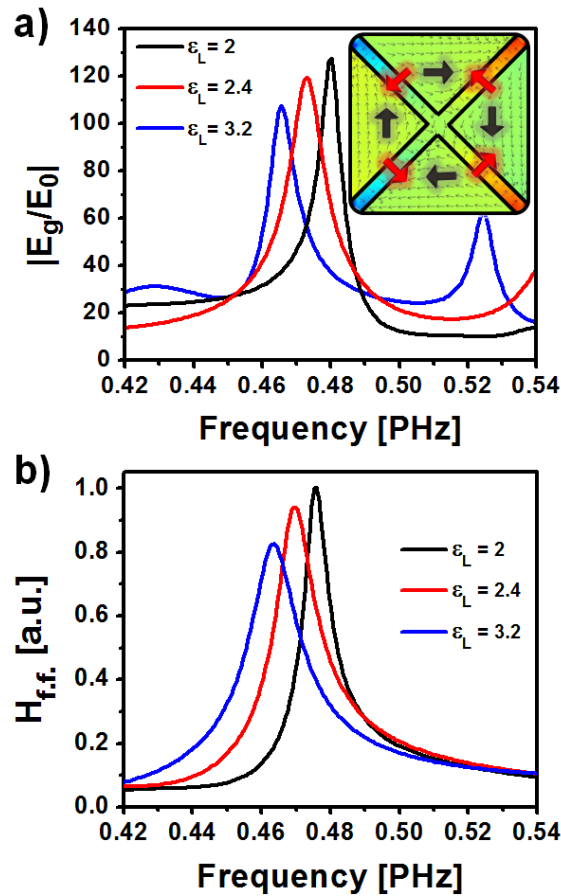


Figure 2 – (Color online) Calculated (a) electric field enhancement at the gap and (b) maximum magnetic far-field for an individual inclusion, varying the loading permittivity  $\epsilon_L$ . The inset shows the electric field distribution in the square-loop plane at its magnetic resonance.

A strong circulating displacement current sustains the artificial magnetism of this geometry. The square-loop provides significant advantages over a loop of nanospheres [11], especially for smaller values of  $g$ , i.e., for thin gaps: a) the presence of tiny elongated gaps ensures uniform and strongly amplified electric field, which may drastically enhance the tunability of the resonance frequency and the nonlinear effects of a Kerr material used as load, consistent with the nanocircuit model of Fig. 1b, in which the gap capacitances are assumed to be *variable*; b) the increased capacitance (1) provided by this specific geometry ensures decreased Q factor of the magnetic resonance, which may provide enhanced robustness to the inherent loss in the metal and increased bandwidth of operation; c) the linear dependence of  $C$  on the loading permittivity ensures large tunability of its magnetic properties.

Figures 2a and 2b show the simulated electric field enhancement factor at the gap and the maximum magnetic far-field, respectively, as a function of frequency for different values of  $\epsilon_L$  for excitation of the single square-loop in Fig. 1a (see [18] for the details of our numerical simulations). Large field enhancement at the gaps may be obtained at the loop magnetic resonance, sensibly tunable by varying  $\epsilon_L$  (Fig. 2a). This large enhancement may drastically amplify the nonlinear properties of Kerr materials used as loads, as we show in the following. Correspondingly, the calculated magnetic far-field in Fig. 2b supports our intuition that the inclusion sustains a strong magnetic dipolar resonance, with similar tuning properties. In this same range of frequencies, the loop geometry sustains a strong electric dipole moment, associated with its plasmonic properties, ensuring that,

when used as a metamaterial inclusion in a periodic array, this geometry may support negative index of refraction in the visible regime.

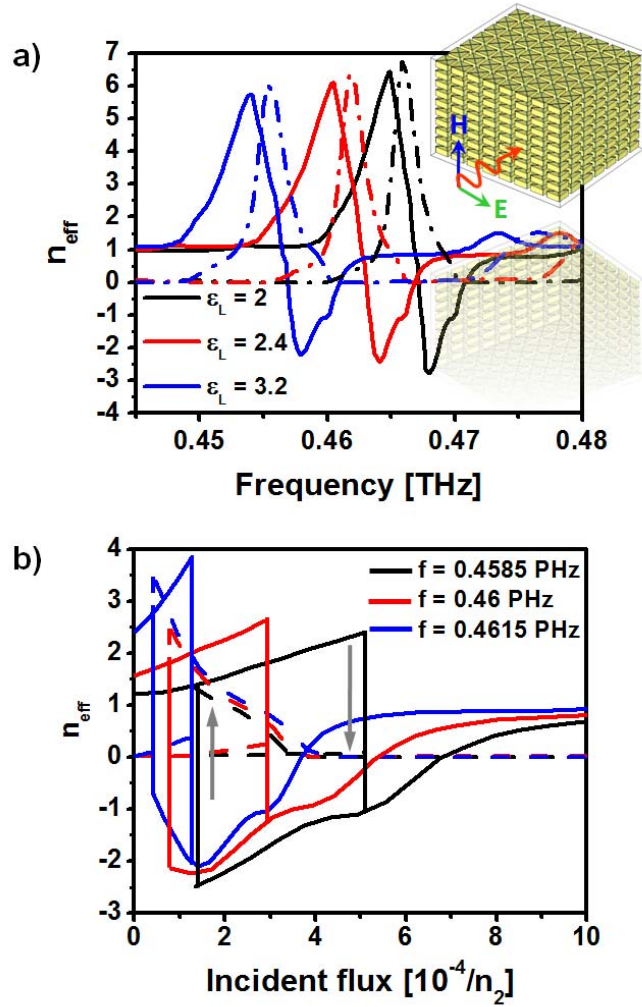


Figure 3 – (Color online) (a) Retrieved effective index of refraction for different values of permittivity  $\epsilon_L$ ; (b) Hysteresis of the index of refraction loaded by Kerr nonlinear materials at various frequencies (real part: solid, imaginary part: dashed).

In Fig. 3a, we have retrieved the effective index of refraction and impedance for a metamaterial slab formed of square-loops, as depicted in the inset, using a technique analogous to [19], i.e., illuminating the slab at normal incidence with



magnetic field polarized along the square-loop axis, and inspecting reflection and transmission coefficients and the field distribution induced at different frequencies inside the slab. The array has a period  $d_x = d_y = 120 \text{ nm}$  in the square-loop plane and  $d_z = 60 \text{ nm}$  in the orthogonal direction, and glass is the host medium. We vary the gap permittivity, verifying that indeed a tunable negative index response may be obtained. The obtained index of refraction may be largely tuned by varying the gap capacitance, as predicted in (1), and the obtained figure of merit  $-\text{Re}[n]/\text{Im}[n]$  for negative index propagation may reach relatively large values (up to 8.5), due to the specific magnetic response of this geometry. We have verified that the extracted parameters are consistent with the phase advance and amplitude decay along the metamaterial slab for several frequencies and load permittivity values, both in the negative and positive index bands. Moreover, our extracted parameters are not affected by the slab thickness, ensuring that they indeed describe the metamaterial macroscopic local properties. This unique metamaterial geometry can combine negative index propagation, large figures of merit and a strong uniform electric field enhancement in the gaps of each inclusion, ideal for the purpose of generating a bistable and self-tunable positive-to-negative index of refraction in the visible.

We generate this effect by loading the inclusions with Kerr nonlinear materials with relative permittivity  $\varepsilon = \varepsilon_L + \chi^{(3)} |E_g|^2$ . The second-order nonlinear refractive index is approximated as  $n(I) = n(0) + n_2 I$ , with low-intensity permittivity  $\varepsilon_L = 2.13$ , typical of nonlinear optical materials;  $I$  is the optical intensity in units

of energy flux and  $n_2$  is the Kerr coefficient [ $\text{cm}^2 / \text{W}$ ]. Figure 3b shows the variation of effective index of refraction with the impinging light intensity for some sample frequencies in the negative index band, calculated combining full-wave numerical simulations with an iterative scheme analogous to [20]. It is seen that the nonlinearly loaded metamaterial supports a strong hysteresis effect in terms of refractive index, which may switch between positive and negative values: for critical values of light intensity, which depend on the frequency of operation and the geometry of the inclusions, the index of refraction may suddenly switch from negative to positive values, and vice versa. The typical hysteresis produced by this bistable operation sustains positive to negative switch as a function of the past excitation history, introducing peculiar memory effects. The strong field enhancement in the gaps, produced by the plasmonic inclusions and the resonant circulating displacement current, ensures that moderate optical intensities may be employed to activate these bistable effects, within the realm of available optical nonlinearities and optical intensity levels, despite the small size of the inclusions. This may have fascinating applications in a variety of metamaterial devices, including tunable optical antennas and filters with novel functionalities or super-resolving lenses with tunable response.

In order to apply these results in a more complex metamaterial setup, we analyze in Fig. 4 the case of a finite metamaterial prism with same geometry as in Fig. 3, excited by a Gaussian beam with magnetic field orthogonal to the plane of the figure. It is evident that positive or negative refraction at the exit of the prism may be achieved for the *same frequency* and *same optical intensity*, simply as a

function of the past history of intensity excitation. We have verified that the hysteresis loop of Fig. 3b may indeed produce a bistable refraction angle at the output face of the prism at different frequencies. In particular, Fig. 4 shows two snapshots in time for the magnetic field distribution at frequency  $f = 459$  THz and optical intensity  $I \approx 4 \times 10^{-5} / n_2$  operating in the upper (a) or lower (b) branch of the bistability diagram of Fig. 3b, i.e., coming from larger or smaller input intensities, respectively. We have assumed here that the metamaterial prism is infinitely extended in the direction orthogonal to the plane of the figure, along the polarization of the impinging magnetic field. Further details of our numerical simulations are available in [18].

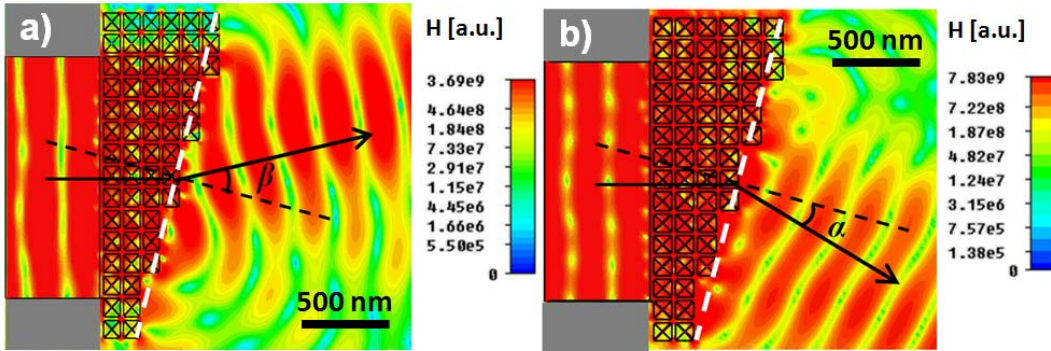


Figure 4 – (Color online) Time snapshots of the magnetic field distribution in the E plane for a finite beam exciting a metamaterial prism composed of square-loops as in Fig. 1 at  $f = 459$  THz with optical intensity  $I = 4 \times 10^{-5} / n_2$ , in the (a) upper and (b) lower bistability branch of Fig. 3b.

The metamaterial prism supports a strong memory effect, for which the transmitted beam may be tilted from positive to negative refraction angles as a function of the past history. Due to some absorption, the negative-index beam is

transmitted slightly unevenly through the prism, with smaller amplitudes in its thicker (upper in Fig. 4) portion. Despite these minor unwanted effects, which may be corrected with lower-loss metamaterials or less thick slabs, a clear positive-to-negative switch of the index of refraction has been obtained. Memory or switch functionalities may be obtained near the transition intensities and for specific frequencies for which the hysteresis loop is small. For an experimental verification, ultra-fast and short-pulsed lasers with high peak intensity may serve as the pump light source [21], avoiding possible bundling and surface melting associated with the loss in the metamaterial. In our vision, optical switching and routing devices based on these concepts may form the basis of novel optical logic and computing systems. Although arguably challenging within current nanofabrication limits, the realization of this metamaterial geometry may be envisioned using advanced lithographic processes (e.g., [22]). To conclude, we have put forward a negative-index metamaterial geometry with strong nonlinear effects, which supports bistable positive-to-negative refractive index, switch and memory effects. The square-loop geometry supports a magnetic-electric resonance with large figure of merit for negative index propagation and large field enhancement at the gaps, boosting optical nonlinearities and ensuring that these effects may be achieved within realistic nonlinear properties of optical materials, i.e., poly( $\beta$ -pinene) or Cu:Al<sub>2</sub>O<sub>3</sub> ( $10^{-9}$ - $10^{-10}$  cm<sup>2</sup>/W) [23], and reasonable input intensities. A bistable, self-tunable and switchable positive-to-negative index of refraction may realize a variety of exciting optical devices, such as memories, switches, self-tunable antennas with directive properties, and imaging devices of

novel generation. This work has been partially supported by Aegis Technologies Inc. with contract number 41-STTR-UTX-0652, NSF with a CAREER award number ECCS-0953311 and an ONR MURI award number N00014-10-1-0942.

- [1] R. Shelby, D.R. Smith, S. Schultz, *Science* **92**, 297 (2001).
- [2] V.G. Veselago, *Sov. Phys. Usp.* **10**, 50914 (1968).
- [3] V. M. Shalaev, *Nat. Photon.* **1**, 41 (2007).
- [4] J.B. Pendry, *Phys. Rev. Lett.* **85**, 3966 (2000).
- [5] J. B. Pendry, D. Schurig, D. R. Smith, *Science* **312**, 1780 (2006).
- [6] B. Gralak, S. Enoch, G. Tayeb, *J. Opt. Soc. Am. A* **17**, 1012 (2000).
- [7] J. D. Jackson, *Classical Electrodynamics* (Wiley, 1998).
- [8] L. Landau, E. M. Lifschitz, *Electrodynamics of continuous media* (Elsevier, 1984); R. Merlin, *Proc. National Acad. Science* **106**, 1693 (2009).
- [9] J. Zhou, T. Koschny, M. Kafesaki, E. N. Economou, J. B. Pendry, C. M. Soukoulis, *Phys. Rev. Lett.* **95**, 223902 (2005).
- [10] G. Shvets, Y. A. Urzhumov, *Phys. Rev. Lett.* **93**, 243902 (2004); A. Alù, N. Engheta, *J. Opt. Soc. Am. B* **23**, 571 (2006); V. A. Podolskiy, A. K. Sarychev, V. M. Shalaev, *J. Nonlinear Opt. Phys. Mater.* **11**, 65 (2002); A. N. Grigorenko, A. K. Geim, H. F. Gleeson, Y. Zhang, A. A. Firsov, I. Y. Khrushchev, J. Petrovic, *Nature* **438**, 335 (2005); N. Fang, H. Lee, C. Sun, X. Zhang, *Science* **308**, 534 (2005).

- [11] A. Alu, A. Salandrino, N. Engheta, *Opt. Exp.* **14**, 1557, (2006); A. Alu, N. Engheta, *Phys. Rev. B* **78**, 085112 (2008).
- [12] D. K. Morits, C. R. Simovski, *Phys. Rev. B* **81**, 205112 (2010).
- [13] N. Zheludev, *Science* **328**, 582 (2010).
- [14] A.A. Zharov, I.V. Shadrivov, Y.S. Kivshar, *Phys. Rev. Lett.* **91**, 037401 (2003); I.V. Shadrivov, Y. S. Kivshar, *J. Opt. A: Pure Appl. Opt.* **7**, 68 (2005); N. Lazarides, G.P. Tsironis, *Phys. Rev. E* **71**, 036614 (2005).
- [15] I. V. Shadrivov, S. K. Morrison, Y. S. Kivshar, *Opt. Expr.* **14**, 9344 (2006); S. O'Brien, D. McPeake, S.A. Ramakrishna, and J.B. Pendry, *Phys. Rev. B* **69**, 241101(R) (2004).
- [16] N. Engheta, A. Salandrino, and A. Alù, *Phys. Rev. Lett.* **95**, 095504 (2005).
- [17] P. B. Johnson, and R. W. Christy, *Phys. Rev. B* **6**, 4370 (1972).
- [18] EPAPS Document: Details of our numerical methods are available in the supplemental material.
- [19] A. Andryieuski, R. Malureanu, A. V. Lavrinenko, *Phys. Rev. B* **80**, 193101 (2009).
- [20] P. Y. Chen, and A. Alù, *Phys. Rev. B* **82**, 235405 (2010).
- [21] M. Danckwerts and L. Novotny, *Phys. Rev. Lett.* **98**, 026104 (2007).
- [22] W. Wu, *Nano Lett.* **8**, 3865 (2008); Z. Li, et al., *Nano Lett.* **9**, 2306 (2009); W. Hu, K. Sarveswaran, M. Lieberman, and G. H. Bernstein, *J. Vac. Sci. Tech. B* **22**, 1071 (2009).

- [23] H. Rajagopalan, P. Vippra, and M. Thakura, *Appl. Phys. Lett.* **88**, 033109 (2006); J. M. Ballesteros, R. Serna, J. Solis, C. N. Afonso, A. K. Petford-Long, D. H. Osborne, and R. F. Haglund, Jr., *Appl. Phys. Lett.* **71**, 2445 (1997).